Dyes and Pigments 181 (2020) 108587

Contents lists available at ScienceDirect

Dyes and Pigments

journal homepage: http://www.elsevier.com/locate/dyepig

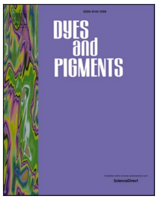

Reversible acidochromism and thermo-responsive luminescence properties of a novel Zn(II)/Eu(III) coordination polymer[☆]

Cristián Cuerva [a,*], Jesús Tapiador [b], Ana E. Sánchez-Peláez [b], M. Carmen Torralba [b], Ángel Gutiérrez [b,**]

[a] BIOSCOPE Research Group, LAQV@REQUIMTE Chemistry Department, NOVA School of Science and Technology, NOVA University Lisbon, 2829-516, Caparica, Portugal

[b] Departamento de Química Inorgánica, Facultad de Ciencias Químicas, Universidad Complutense, 28040, Madrid, Spain

A R T I C L E I N F O

Keywords:
Acidochromism
Sensors
Salen-type compounds
Lanthanides
Coordination polymers

A B S T R A C T

A new Zn(II)/Eu(III) compound with the *N,N′*-ethylenebis(5-carboxysalicylideneamino) ligand (H_4Salendc) has been synthesised and its photophysical behaviour studied. This species, [Zn(Salendc)Eu(CH_3COO)(DMSO)]·xH_2O·0.5CH_3CN (x = 3.5–4), has been characterised by XRD, XEDS and SEM and HTEM microscopies. Experimental results suggest the formation of a one-dimensional polymeric compound. The compound behaves as a luminescent material in the solid state. Moreover, it exhibits acidochromic properties upon the addition of a few drops of HCl and in the presence of its vapours. The emission intensity of the bands attributed to the Eu(III) ion can be also modulated by the temperature and by the presence of water, so that this species is a good candidate for its use as a luminescent acid, temperature and water sensor.

1. Introduction

The fascinating photoluminescence of lanthanide(III) complexes make them very interesting materials with a great potential for photonic applications, such as light-emitting diodes (LED) or amplifiers for optical displays and sensing devices [1–5]. The luminescence properties of polynuclear lanthanides are usually increased using chromophore ligands to induce an efficient emission because they transfer the absorbed energy toward the lanthanide ion [1]. One of the main classes of chromophores investigated corresponds to Schiff bases. In addition, Schiff base ligands have developed great interest because of their multiple applications in catalysis, in bioinorganic systems or as antitumoral drugs [6].

The Schiff base environment protects, in many cases, the Ln(III) centre of the solvent molecules, improving the luminescence properties of the complexes. One of the best known multidentate ligands is the Schiff base H_2salen, *N,N′*-ethylenebis(salicylideneamino), and its derivatives. These tetradentate or multidentate ligands are rather versatile and form complexes with lanthanides providing a wide structural variety, since they are flexible ligands that can show different coordination modes. In these complexes, the *salen*-type ligands stabilise the metal centres and act as an antenna for the luminescence of the lanthanide ion. The stoichiometry and structures of the multimetallic compounds depend on diverse factors such as the type of Schiff base used, the ionic radius of the lanthanide, the counterion nature, the pH of the medium or the type of synthesis [7].

The control over the stoichiometries and structures of heterometallic polynuclear complexes containing transition metals and/or lanthanide metal ions is a challenge because of the varied coordination numbers and environments showed by the lanthanide cation. In addition, modifications over the ligand can also influence on the formation of the polynuclear entities affecting the final complex properties. Several *d-f* polynuclear complexes have been investigated giving rise to the formation of Yb(III), Nd(III), Ho(III) or Er(III) derivatives with emissions in the range of about 900–1600 nm, close to near infrared (NIR), being adequate for biotechnological applications and in laser systems [8].

On the other hand, Eu(III) complexes exhibit a high quantum yield and a long-live emission, which make them suitable candidates for the preparation of novel advanced functional materials with sensorial abilities. It is well-known that the coordination of water, to complete the

---

[☆] Dedicated to Professor José Antonio Campo Santillana, in memoriam.

[*] Corresponding author.

[**] Corresponding author.

E-mail addresses: c.alaiz@fct.unl.pt (C. Cuerva), agalonso@ucm.es (Á. Gutiérrez).

https://doi.org/10.1016/j.dyepig.2020.108587
Received 9 April 2020; Received in revised form 25 May 2020; Accepted 25 May 2020

coordination sphere for example, can cause a quenching of the Eu(III) emission bands by the antenna effect blocking [9]. As a result, only intraligand transitions are allowed in the complex. This behaviour has been reported in the literature as a strategy to detect water *via* luminescence spectroscopy in certain solvents or humid environments [10–12]. However, it has also allowed to developed novel Eu(III) complexes with stimuli-responsive properties. The application of an external stimulus can induce the establishment of new intermolecular interactions, and coordinated water can be replaced by other chromophore ligands in order to revival the antenna effect [13–15].

In this work, a new polymeric Zn(II)/Eu(III) compound with a flexible dicarboxylic *salen*-type ligand, *N,N′*-ethylenebis(5-carboxysalicylideneamino), H_4Salendc, has been obtained and its photophysical behaviour studied. The *salen* compound used as the ligand has been strategically functionalised with terminal carboxylic groups to favour the formation of coordinative –COO···Eu···OOC– bonds. Interestingly, it is possible to break and form again these short contacts upon exposure to several external stimuli, which originates dramatic changes in the luminescence properties of the complex. Structure/properties relationships have been studied in deep to understand the mechanisms of these processes; results could be of great interest for potential application in the field of thermo and acid sensors.

2. Experimental section

2.1. Materials and physical measurements

All chemicals were purchased from Aldrich and were used without further purifications.

Elemental analysis (carbon, hydrogen and nitrogen) were carried out by the Microanalytical Service of the Universidad Complutense de Madrid (UCM) using a LECO CHNS-932 analyser. FTIR spectra (4000-650 cm^{-1}) of solid powder samples were recorded using a Perking Elmer spectrophotometer with a universal ATR accessory and FTIR KBr-dispersion spectra (4000-400 cm^{-1}) were recorded using a THERMO NICOLET 200 spectrophotometer. ^1H NMR spectra of the ligand were collected in the UCM Nuclear Magnetic Resonance Service using a Burker AVIII300 (300 MHz) spectrophotometer. The thermogravimetric data were obtained on a Perkin Elmer Pyris 1 TGA using an open pan, which was purged with N_2, operating at a heating rate of 5–10 °$Cmin^{-1}$. Electron microscopy studies were carried out either in a JEOL JEM-2100HT transmission electron microscopy (TEM) operating with an accelerating voltage of 200 kV or in a JEOL JEM GRAND ARM300cF operating at 60 kV with a resolution of 0.5 Å; scanning electron microscopy (SEM) was performed using a JEOL JSM 6335 FEG electron microscope operating at 5 kV. Chemical composition analysis was also performed on the JEOL JEM-2100HT electron microscope using energy dispersive X-Ray spectroscopy (XEDS). X-Ray diffraction patterns were recorded in an X'PERT-MPD diffractometer working with monochromatic Cu Kα radiation at 45 kV and 40 mA.

Variable-temperature magnetic susceptibility measurements in the temperature range of 2–300 K were performed on a Quantum Design MPMSXL SQUID magnetometer using a constant magnetic field of 0.5 T. All susceptibility data were corrected for the diamagnetic contribution of the sample holder, while the molar diamagnetic corrections from the sample were calculated using the Pascal constants.

The excitation and emission spectra were recorded on a Horiba Jobin-Yvon Fluoromax-4 spectrofluorimeter using a fibre-optics device connected to the spectrofluorimeter, exciting the solid compounds at the appropriated wavelength. The emission spectra at variable temperature were obtained by heating the samples over a hotplate with temperature control.

2.2. Synthesis of $H_4Salendc.0.25H_2O$

This ligand has been synthesised following the reported procedure for the analogous phenylene derivative [16]: to a stirred suspension of 3-formyl-4-hydroxybenzoic acid (0.668 g, 4 mmol) in 50 mL of MeOH a solution of ethylenediamine (135 μL, 2 mmol, 99%) in 10 mL of methanol was dropwise added. The mixture changed to yellow colour and it was refluxed for 4 h. After cooling at room temperature, a yellow solid was obtained that was filtered off, washed several times with cold MeOH and dried under vacuum. Yield: 74%.

Anal. Calc. (%) for $C_{18}H_{16}N_2O_6.0.25H_2O$: C, 59.9; H, 4.61; N, 7.76. Found: C, 59.9; H, 4.49; N, 7.68. IR (KBr pellets, cm^{-1}): 2906 m, 2789 m, 2650 m, 2553 m, 2210w, 1635s, 1589 m, 1568 m, 1524 m, 1484 m, 1450 m, 1361s, 1316 m, 1281s, 1235w, 1215w, 1196w, 1180w, 1123w, 1112w, 1077w, 1033 m, 1012w, 981w, 932w, 868w, 844w, 819w, 789s, 685 m, 637 m, 536w, 460w, 428 m. ^1H NMR (DMSO-d_6, ppm): 3.93 (s,4H), CH_2; 6.0 (s,2H), HO–Ph; 6.83 (d,2H), Ph; 7.81 (m,2H), Ph; 8.01 (m,2H), Ph; 8.68 (s,2H) HC=N.

2.3. Synthesis of $[Zn(Salendc)Eu(CH_3COO)(DMSO)]\cdot xH_2O\cdot 0.5CH_3CN$ ($x = 3.5–4$)

To a warm yellow suspension of H_4Salendc (0.250 g, 0.69 mmol) in 10 mL of DMSO, 40 μL of Et_3N (0.29 mmol, 0.726 g/cm^3, 99%) were added, followed by a solution of $Zn(CH_3COO)_2\cdot 2H_2O$ (0.152 g, 0.69 mmol) in 5 mL of DMSO. After 5 min of stirring, $Eu(NO_3)_3\cdot 5H_2O$ (1.039 g, 2.43 mmol) was added, and the mixture was refluxed for 30 min, in order to dissolve completely the europium salt. The resulting yellow solution was cooled to room temperature and the solvent was slowly evaporated for two weeks, until a yellow powder is formed. The solid was filtered off, washed several times with acetonitrile and dried in vacuum. Yield: 57%.

Anal. Calc. (%) for $C_{22}H_{21}EuN_2O_9SZn.3.75H_2O.0.5CH_3CN$: C, 34.75; H, 3.80; N, 4.41. Found: C, 34.74; H, 3.81; N, 4.37. IR (KBr pellets, cm^{-1}): 3388br, 2914w, 1641s, 1606s, 1553s, 1510 m, 1432 m, 1398vs, 1381vs, 1314 m, 1248w, 1190w, 1130 m, 1016 m, 954w, 850w, 793 m, 745w, 689 m, 646 m, 515w.

3. Results and discussion

3.1. Synthesis and structural characterisation

The ligand was obtained by condensation of ethylenediamine with 3-formyl-4-hydroxybenzoic acid in a 1:2 ratio under refluxing conditions in methanol, following the reported procedure for the analogous phenylene derivative [16]. The synthesis of $[Zn(Salendc)Eu(CH_3COO)(DMSO)]\cdot xH_2O\cdot 0.5CH_3CN$ ($x = 3.5–4$) was carried out in two steps by the "one pot synthesis" method. In a first step, the precursor $[Zn(Salendc)]^{2-}$ was formed by reaction of the deprotonated ligand, $Salendc^{4-}$, with $Zn(CH_3COO)_2\cdot 2H_2O$. A small quantity of base (Et_3N) must be present in the reaction mixture to help the carboxylate deprotonation; however, the presence of the base seems to have a catalytic role since it is not necessary the addition of a stoichiometric amount for the reaction to proceed. The complexation of the zinc ion is proposed due to the solubilisation of the *salen* ligand. In the second step, addition of $Eu(NO_3)_3\cdot 5H_2O$ to the precursor solution afforded the final compound. The solid was obtained by slow evaporation of the solvent. The obtained derivative presents very low solubility in common organic solvents, suggesting that a coordination polymer has been formed (Scheme 1).

The thermogravimetric study of this compound shows successive and ill-defined weight losses on heating between 50 and 760 °C (Fig. S1). A first step between 50 and 220 °C corresponds to a weight loss of 12% that can be attributed to the removal of the crystallisation solvent molecules. This result, along with the analytical data, allows an estimation of the solvent content corresponding to an average of 3.5–4 water molecules and half acetonitrile per metal complex (11% weight loss). Upon further heating, the metal complex decomposes with a 59% weight loss (expected 58% loss) and the final products are identified by X-ray diffraction as $Eu_2(SO_4)O_2$ and ZnO in an approximate 1:1 metal

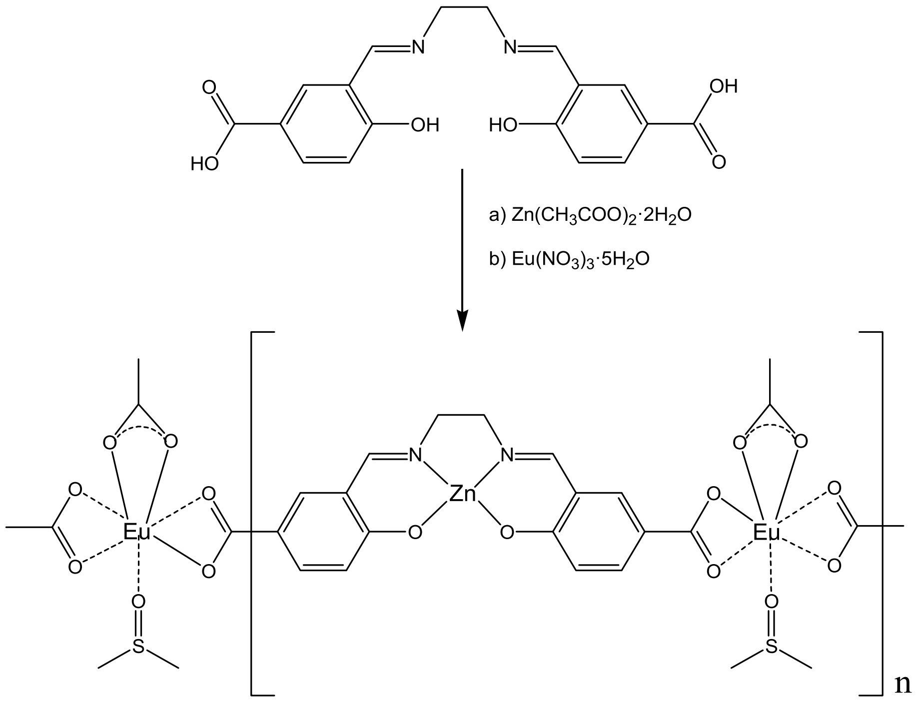

Scheme 1. Proposed coordination environments for the metal ions in the coordination complex.

ratio. The sulphate ion comes from the oxidation of part of the DMSO that is not easily removed due to its high boiling point. In a parallel experiment, when the dinuclear complex is washed with MeOH, the coordinated DMSO molecule is displaced and the thermogravimetric residue of this new sample corresponds to a mixture of Eu_2O_3 and ZnO.

The IR spectrum of H_4Salendc exhibits several OH stretching vibration bands in the 3100–2500 cm^{-1} region, which is typical of H-bonded carboxylic acids, along with a ν(C=O) band at 1635 cm^{-1} and a ν(C–O) band at 1361 cm^{-1}, also characteristic of the dimerised carboxylic group. Other bands at 1589, 1281 and 789 cm^{-1} can be respectively attributed to the ν(C=N), $\nu(C\text{–}O_{phenoxo})$ and $\delta(CH)_{ring}$ and they are characteristic of the *salen*-type ligands [17].

When the metal complex is formed, the spectrum is modified in consonance with the coordination of the metal ions. A broad ν(O–H) band, attributed to either crystallisation or coordinated water, is observed at 3388 cm^{-1}. The ν(C=O) band at 1641 cm^{-1} along with the ν(C–O) band at 1381 cm^{-1} can be attributed to the *salen* carboxylate group, whose frequencies are slightly shifted to higher values due to the coordination to the europium ion. The other pair of carboxylate stretching bands, at 1553 and 1398 cm^{-1}, can be respectively assigned to asymmetric and symmetric stretching modes of the acetate group, which is probably coordinated in a chelate fashion to the europium ion.

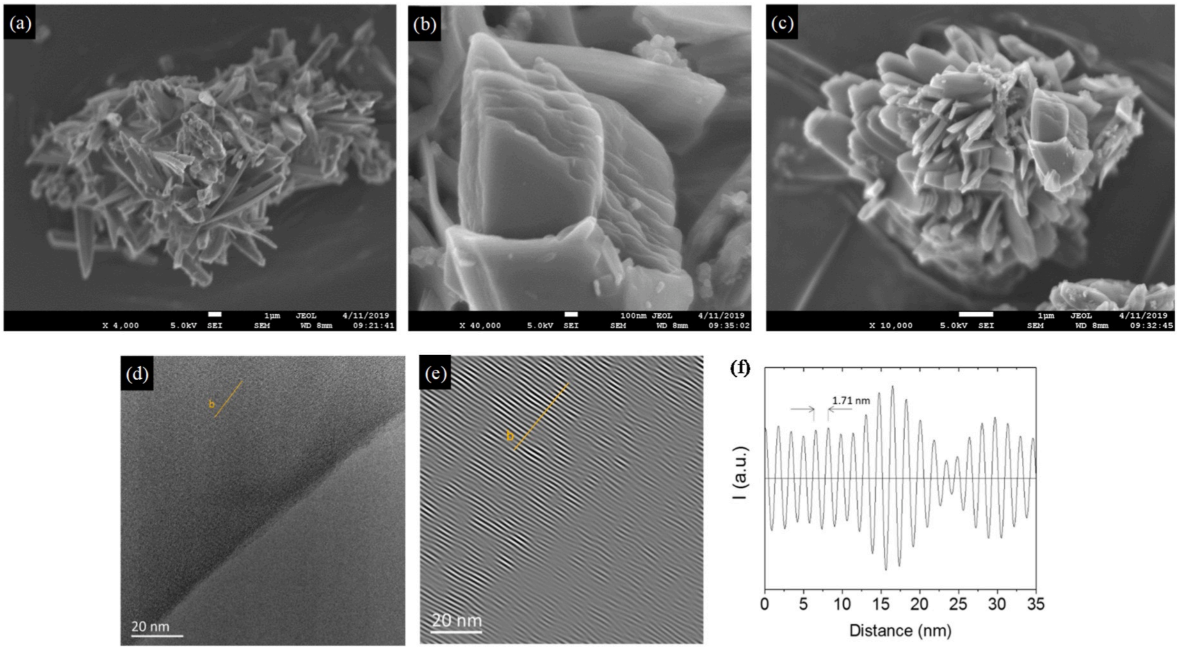

Fig. 1. (a,b,c) SEM images of the Zn(II)/Eu(III) complex; (d) TEM images of the Zn(II)/Eu(III) complex. (e) Filtered TEM image; (f) Plot of interplanar spacing along the yellow line in the previous image.

The $\nu(C{=}N)$ and $\nu(C\text{–}O_{phenoxo})$ stretching bands of the *salen* ligand are shifted to higher values, 1606 and 1314 cm^{-1}, respectively. This shift is indicative of the metal coordination in the complex cavity. Finally, there is one broad and medium intensity band at 1016 cm^{-1} that can be assigned to the $\nu(S{=}O)$ of a DMSO molecule coordinated to the europium ion (Fig. S2) [18].

Due to the impossibility of getting good quality crystals to solve the structure of this complex, an electron microscopy study of the sample has been performed. The SEM images (Fig. 1a–c) show homogeneous needle shape crystals that are formed by thin sheets stacked together. These crystals are unstable under the electron beam and decompose after a short period of time. It is possible, however, to get some TEM images (Fig. 1d) before decomposition has taken place. A filtering of the image allows measuring an interplanar spacing of 17.1 Å (Fig. 1e and f), which is consistent with twice the d-spacing of the most intense peak (10.3°, 8.59 Å) found in the X-ray diffractogram (Fig. S3).

The crystals have been analysed under the microscope using the XEDS technique in several areas of the sample (Fig. 2). The data indicate that, on average, the Eu/Zn ratio is 1:1. There is also a small signal corresponding to the presence of sulfur, but in a Eu/S ratio of 4:1, suggesting that the DMSO coordinated to the rare earth ion is being lost under the electron beam, a fact that can correspond to the low sample stability under these conditions. By contrast, the SEM analysis of the sample surface shows a higher proportion of sulfur atoms with an approximate ratio S:Zn:Eu of 3:1:1, indicative of the DMSO would be migrating to the surface prior to the crystal decomposition under the electron beam. Additionally, the XEDS of a sample washed with methanol does not show the signal corresponding to sulfur atoms, supporting the previous observation of the DMSO removal by the methanol from the coordination sphere of the europium ion.

The electron microscopy data can bring some light on the structure of the complex when compared to the known structures of the similar dicarboxylate *salen*-type ligands in the CSD database. These data show a distance of 17–19 Å between metal atoms coordinated to the carboxylic groups in both ends of the ligand [19–21]. This distance is dependent on the size of the metal ion linked to the carboxylate and on the flexibility of the central diimide portion of the *salen* ligand, being longer with rigid moieties, such as phenylene groups. This similitude allows us to propose the formation of one-dimensional chains …–Eu–OOC–(ZnSalendc)–COO–Eu–OOC–… in the crystal, being the Eu(III)–Eu(III) distance the responsible for the 17.1 Å spacing observed in the electron microscopy images. The formation of a polymeric species would also agree with the extremely low solubility of this compound.

The magnetic susceptibility of the complex has been measured in the temperature range of 2–300 K, and results are shown in Fig. 3. The observed χT values steadily decrease from 0.88 cm^{3}Kmol^{-1} at 300 K to a minimum value of 0.008 cm^{3}Kmol^{-1} at 2 K. Since the Zn(II) ion is diamagnetic, the observed susceptibility should be attributed to the europium ion. The usual behaviour of the Eu(III) is to populate only the ground level ($4f^6$, $J = 0$, $S = 3$, $L = 3$, $^7F_0$), leading to a diamagnetic ground state. The observed behaviour must correspond to a thermal population of the low level excited states; these levels will depopulate on cooling leading to a final diamagnetic state when the temperature approaches the zero.

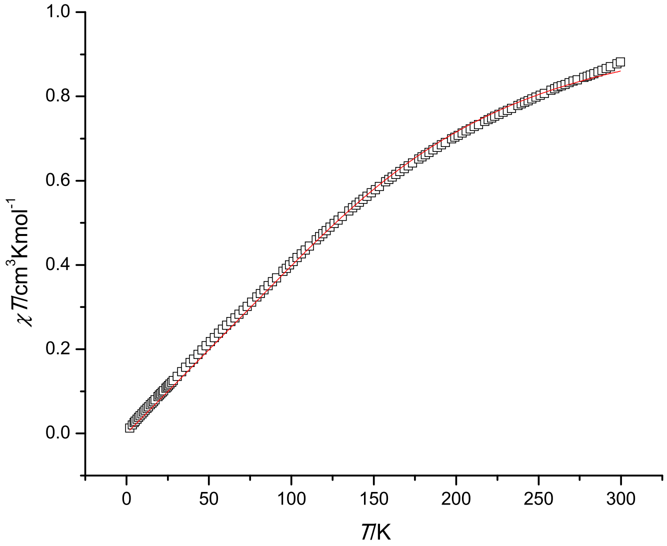

Fig. 3. Temperature dependence of χT for the Zn(II)/Eu(III) complex. The solid line represents the best fit using the parameters described in the text.

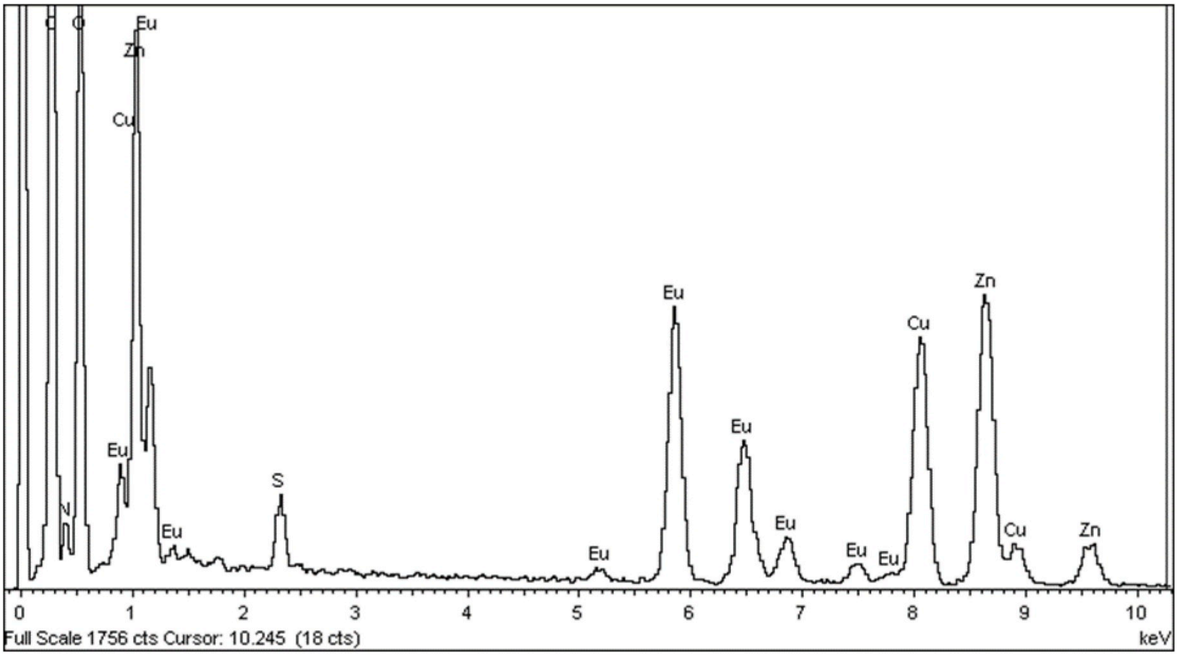

Fig. 2. XEDS spectrum of the Zn(II)/Eu(III) complex using Cu standard.

The analytical expression to fit the experimental data takes into account the seven first energy levels $^7F_0$, $^7F_1$, $^7F_2$, $^7F_3$, $^7F_4$, $^7F_5$, $^7F_6$ [22].

$$\chi = \frac{N\beta^2}{3\lambda}\,\frac{24 + (13.5w - 1.5)e^{-w} + (67.5w - 2.5)e^{-3w} + (189w - 3.5)e^{-6w} + (405w - 4.5)e^{-10w} + (742,5w - 5.5)e^{-15w} + (1228.5w - 6.5)e^{-21w}}{1 + 3e^{-w} + 5e^{-3w} + 7e^{-6w} + 9e^{-10w} + 11e^{-15w} + 13e^{-21w}}$$

where $w = \lambda/kT$ and β and k have their usual meanings. The fitting parameter $\lambda = 391\ \mathrm{cm}^{-1}$ indicates the energy difference between the ground and first excited states and its value is comparable to that found between the $^5D_0 \rightarrow {}^7F_0$ (578 nm) and $^5D_0 \rightarrow {}^7F_1$ (590 nm) transitions observed in the electronic spectrum of this compound ($\lambda = 352\ \mathrm{cm}^{-1}$) (see the luminesce behaviour section).

3.1.1. *Luminescence behaviour*

Fig. 4a displays the excitation and emission spectra of the Zn(II)/Eu(III) complex in the solid state. As observed, the excitation band attributed to singlet metal-to-ligand charge transfers between the Zn atom and the *salen*-type ligand appears centred at 400 nm, and the corresponding emission band is located at around 443 nm. In addition, the typical sharp band of the Eu(III) ion associated with the $^5D_0$-$^7F_2$ transition is clearly detected at 614 nm, as well as the remaining ones originated from the $^5D_0$-^7F_J (J = 0, 1, 3 and 4) transitions, which appear at 578, 590, 652 and 700 nm, respectively [23]. As a result of these features, the complex emits red light under exposure to UV light (Fig. 4b). Unfortunately, the new complex forms a poorly soluble coordination polymer and thus, further characterisation in solution cannot be conducted.

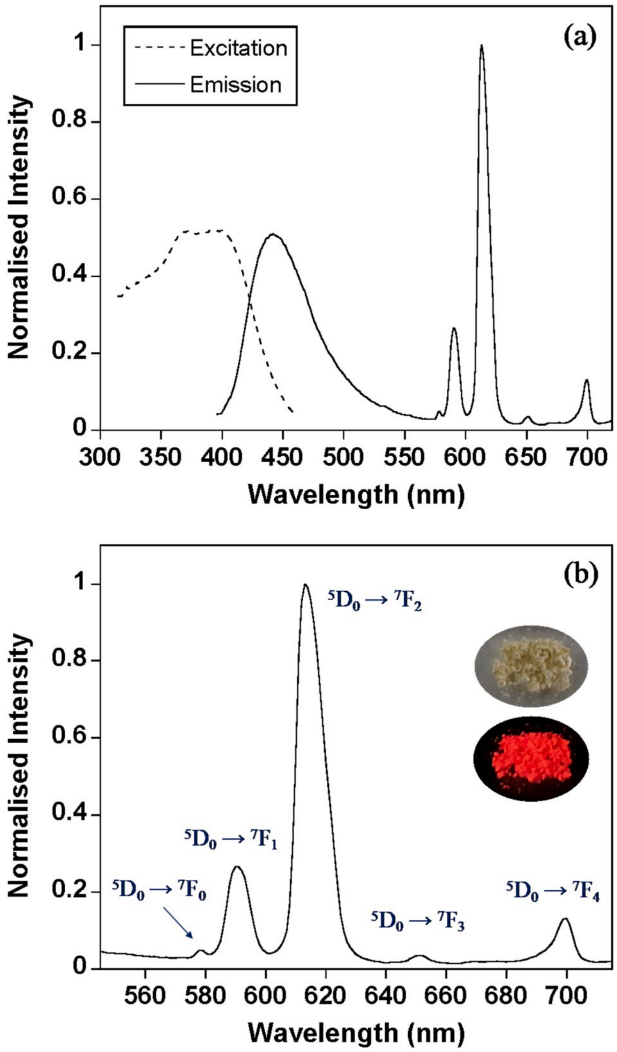

Fig. 4. (a) Normalised excitation and emission spectra of the Zn(II)/Eu(III) complex recorded in the solid state at room temperature. (b) Magnification of the emission spectrum showing the $^5D_0$-^7F_J (J = 0–4) transitions from Eu(III) ion. Inset displays images of the complex in the solid state taken with the naked eye and upon UV light ($\lambda_{exc} = 365$ nm).

Temperature-dependent studies were performed in order to check the fluorescence response by the effect of this external stimulus. As expected, the increase of temperature from 25 to 90 °C causes a progressive quenching of the emission bands, in agreement with the presence of thermally-activated non-radiative processes (Fig. 5a) [24]. The quenching effect is similar for all the emission bands, regardless their nature. Otherwise, since the reached temperature is not enough for thermal decomposition to occur (see TGA experiments), the initial red emission can be practically recovered by cooling back the sample to room temperature (Fig. 5b). The intensities at the emission maximum of the bands centred at 443 and 614 nm as a function of temperature in both heating and cooling cycles are plotted in Fig. 6. Note that, upon cooling, the emission intensity of the band associated with the $^5D_0$-$^7F_2$ transition of the Eu(III) ion ($\lambda_{em} = 614$ nm) is quickly recovered at each temperature, whereas the blue emission from the Zn(II) ion ($\lambda_{em} = 443$ nm) is slower than that recorded on heating, especially at lower temperatures.

Although suitable single-crystals for XRD studies could not be obtained, all data seem to indicate that the Eu(III) ion is coordinated *via* the carboxylate groups of two neighbouring molecules, generating a polymer complex in which the coordination sphere around the Eu(III) ion presents labile coordinated ligand such as DMSO. To demonstrate this fact, two experiments were performed taking into account the luminescence behaviour of the compound. On the one hand, some few drops of water were added over the solid sample and then, the emission spectrum was recorded. Note that the emission intensity of the bands associated with the $^5D_0$-^7F_J transitions of the Eu(III) ion remarkably decreases, and the red emission of the compound is quenched (Fig. 7). To understand this fact, we have to keep in mind that non-radiative transitions are also vibrational-activated processes, so that the typical emission of the Eu(III) complexes strongly depends on the coordination environment. Water molecules have easy access to the coordination sphere of Eu(III) in this compound by displacement of coordinated DMSO and, consequently, energy is transferred in form of O–H vibrations, originating non-radiative processes that result in the luminescence quenching effect observed [25]. Alternatively, as it has been previously commented, repeated washing with methanol displaces the DMSO from the europium coordination sphere, quenching the luminescence behaviour of the complex.

On the other hand, we also explore the luminescence response of the complex after treatment the solid with a concentrated solution of HCl (12 M). As shown in Fig. 8a, the addition of just only two drops of this acidic solution again produces a total quenching of the red emission attributed to the Eu(III) ion. Most likely, protonation of the carboxylate groups causes the rupture of the –COO···Eu···OOC– bonds, and water molecules are coordinated to Eu(III). Concomitantly, the band involving the Zn(II) centre and the *salen*-type ligand is red-shifted from 443 nm to

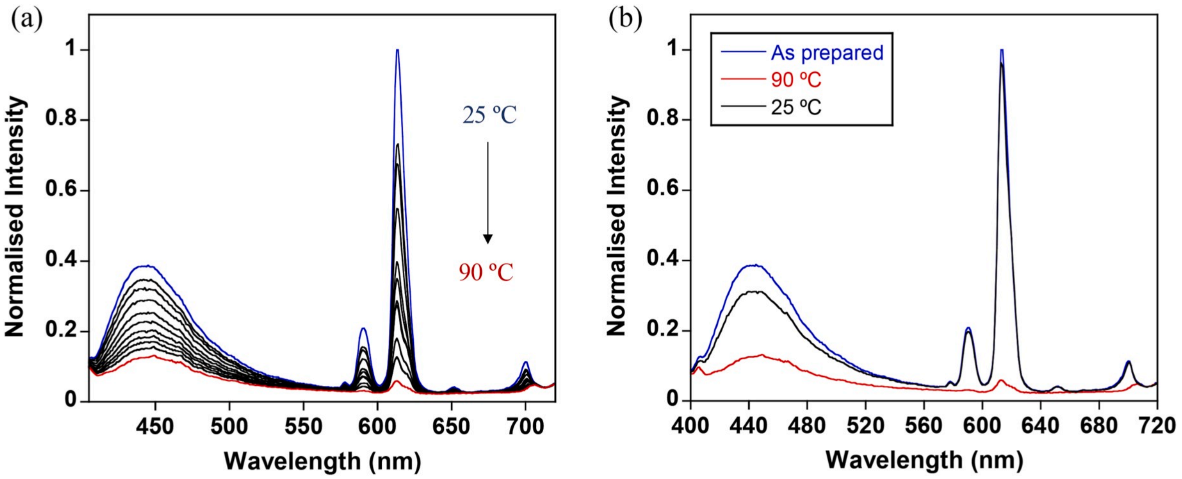

Fig. 5. (a) Normalised emission spectra recorded in the solid state at variable temperature. (b) Normalised emission spectra at selected temperatures during the heating and cooling processes.

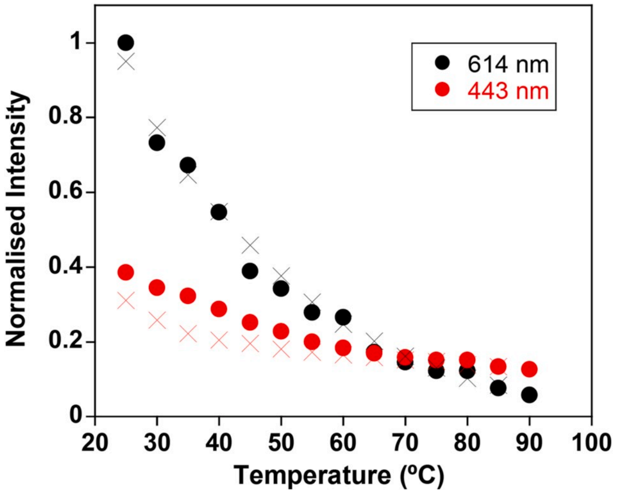

Fig. 6. Emission intensity as a function of temperature read at 443 and 614 nm during the heating (circles) and cooling (crosses) cycles.

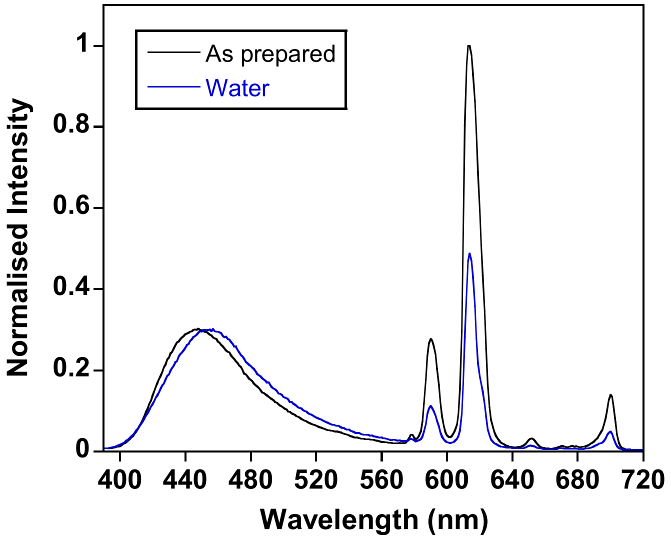

Fig. 7. Emission spectra of the complex as prepared and after the addition of some drops of water.

484 nm and the emission intensity is also increased, so that the complex displays now an intense blue emission (Fig. 8b). Similar features have been previously reported for other complexes with π-conjugated ligands, associating this effect to energy changes in the frontier orbitals as a result of protonation [26]. Moreover, this luminescence response is not only produced by the action of concentrated HCl in solution, but also by the presence of its vapours (Fig. S4). Although experiments were performed in the solid state and mobility is reduced, protonation/deprotonation can easily occur in the surface of the compound by adsorption of HCl molecules [27,28]. Additional experiments were performed in several acidic media by exposure of the sample to sulfuric, nitric and acetic acids, but no remarkable changes in the fluorescence emission were detected.

From the point of view of the potential application of this material as a sensor of HCl in highly acid media, we were also interested in exploring if deprotonation can again favour the establishment of contacts between the Eu(III) ion and the carboxylate groups because it could allow to recover the initial emission and reuse the material. For this purpose, several drops of an ammonia solution (25%) were added over the solid. Interestingly, the emission spectrum shows a similar pattern than that of the complex as prepared (Fig. 8a), and the resulting solid emits an orange light as demonstrated in Fig. 8b, which confirms the regeneration of the –COO···Eu···OOC– bonds and the recovery of the polymer complex. The permutable ability of these contacts has been evaluated by submitting the complex to successive cycles of treatment with HCl and NH_3 solutions. Results show good reversibility, and no degradation is observed during at least 6 cycles. In fact, the emission maximum at 484 nm is progressively blue-shifted after each treatment with NH_3, reaching values near to those found in the initial solid (Fig. 8c). Similar results were obtained by exposure of the complex to ammonia vapours (Fig. S5).

4. Conclusions

A new derivative containing Zn(II) and Eu(III) ions coordinated to a dicarboxilate *salen*-type ligand has been obtained and characterised. The observed data suggests that the zinc ion would coordinate to the N_2O_2 central cavity of the *salen* ligand while the europium ion is bonded to the carboxylate groups of several Salendc^{4-} ligands, leading to the formation of a polymeric structure. The europium coordination is completed by the presence of acetate anions and dimethylsulfoxide molecules. The latter seem to be essential for the luminescence behaviour of the europium ion, since the treatment of the complex with water or excess methanol quenches the emission by displacement of the DMSO from the europium coordinative sphere.

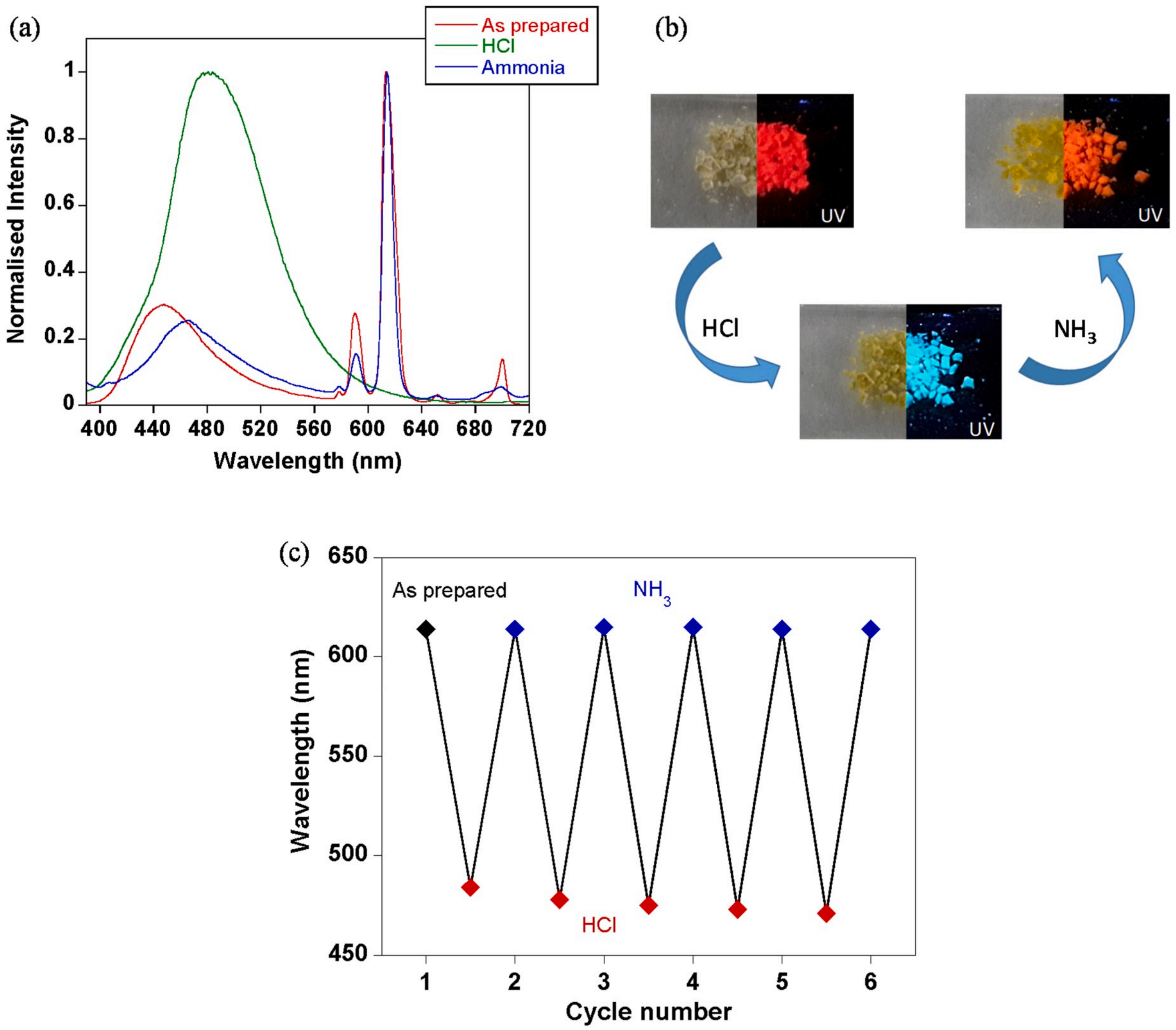

Fig. 8. (a) Emission spectra of the Zn(II)/Eu(III) complex recorded as prepared, after adding some drops of a concentrated HCl solution (12 M), and upon treatment with ammonia solution (25% in water). (b) Images showing the acidochromic behaviour of the complex, taken with the naked eye and under UV light (λ_{exc} = 365 nm). (c) Wavelength at the emission maximum after successive cycles of treatment with HCl and NH$_3$ solutions.

The new complex behaves as a luminescent material, emitting a red light in the solid state as a result of the $^5D_0$-^7F_J transitions from the Eu (III) ion. The activation of non-radiative processes by the effect of temperature causes a quenching of the emission, which can be recovered after back to initial conditions. The complex also exhibits acidochromic properties because of the rupture of the –COO···Eu···OOC– bonds by protonation of the terminal carboxylate groups located in the ligand. The chromic behaviour can be reverted without causing degradation of the sample, this feature demonstrating the usefulness of the material for application as sensor of HCl.

Declaration of competing interest

The authors declare that they have no known competing financial interests or personal relationships that could have appeared to influence the work reported in this paper.

CRediT authorship contribution statement

Cristián Cuerva: Investigation, Visualization, Supervision, Writing - original draft. **Jesús Tapiador:** Investigation, Visualization. **Ana E. Sánchez-Peláez:** Conceptualization, Investigation, Supervision, Writing - review & editing. **M. Carmen Torralba:** Investigation, Visualization, Writing - review & editing. **Ángel Gutiérrez:** Supervision, Writing - review & editing, Funding acquisition.

Acknowledgements

This work was supported by the Associate Laboratory for Green Chemistry – LAQV, which is financed by national funds from FCT/MCTES (UIDB/50006/2020), and the PROTEOMASS Scientific Society. C. Cuerva acknowledges the Spanish Foundation Alfonso Martín Escudero for his postdoctoral fellowship.

Appendix A. Supplementary data

Supplementary data to this article can be found online at https://doi.org/10.1016/j.dyepig.2020.108587.

References

[1] Bünzli J-CG. On the design of highly luminescent lanthanide complexes. Coord Chem Rev 2015;293–294:19–47.
[2] Wang K, Ma Y, Tang H. Lanthanide coordination polymers as luminescent sensors for the selective and recyclable detection of acetone. Crystals 2017;7:199–208.
[3] Zhao S-N, Wang G, Poelman D, Van Der Voort P. Luminescent lanthanide MOFs: a unique platform for chemical sensing. Materials 2018;11:572–98.
[4] Hasegawa Y, Kitagawa Y. Thermo-sensitive luminescence of lanthanide complexes, clusters, coordination polymers and metal–organic frameworks with organic photosensitizers. J Mater Chem C 2019;7:7494–511.

[5] Yao Y, Yin H-Y, Ning Y, Wang J, Meng Y-S, Huang X, Zhang W, Kang L, Zang J-L. Strong fluorescent lanthanide salen complexes: photophysical properties, excited-state dynamics, and bioimaging. Inorg Chem 2019;58:1806–914.

[6] Hazra S, Paul A, Sharma G, Koch B, Guedes da Silva MFC, Pombeiro AJL. Sulfonated Schiff base Sn(IV) complexes as potential anticancer agents. J Inorg Biochem 2016;162:83–95.

[7] Fu G, Li B, Guo J, Liu L, Zhang K, Feng W. OAc–-dependent self-assembly of luminescent homoleptic [Ln$_9$(OH-Salen)$_5$(OH)$_4$(OAc)$_{10}$] and {[Ln$_6$(OH-MeO-Salen)$_5$(OH)(OAc)$_2$(H$_2$O)$_2$]·(OAc)} complexes. Cryst Growth Des 2018;18:1020–9.

[8] Wang C, Wang S, Bo L, Zhu T, Yang X, Zhang L, Jiang D, Chen H, Huang S. Synthesis, crystal structures and NIR luminescence properties of binuclear lanthanide Schiff Base complexes. Inorg Chem Commun 2017;85:52–5.

[9] Song L, Wu Y-W, Chai W-X, Tao Y-S, Jiang C, Wang Q-H. Fluorescence quenching of a europium coordination compound for the detection of trace amounts of water: uncovering the response mechanism by structural confirmation. Eur J Inorg Chem 2015;2015:2264–71.

[10] Gao F, Luo F, Chen X, Yao W, Yin J, Yao Z, Wang L. Fluorometric determination of water in organic solvents using europium ion-based luminescent nanospheres. Microchim Acta 2009;166:163–7.

[11] Knall AC, Tscherner M, Noormofidi N, Pein A, Saf R, Mereiter K, Ribitsch V, Stelzer F, Slugovc C. Nonradiative deactivation of europium(III) luminescence as a detection scheme for moisture. Analyst 2012;137:563–6.

[12] Park JY, Suh M, Kwon YU. Humidity sensing by luminescence of Eu(III)-doped mesoporous silica thin film. Microporous Mesoporous Mater 2010;127:147–51.

[13] Raj DBA, Biju S, Reddy MLP. One-, two-, and three-dimensional arrays of Eu^{3+}-4,4,5,5,5-pentafluoro-1-(naphthalen-2-yl)pentane-1,3-dione complexes: synthesis, crystal structure and photophysical properties. Inorg Chem 2008;47:8091–100.

[14] Gaspar RDL, Fortes PR, Mazali IO, Sigoli FA, Raimundo Jr IM. Optical temperature sensors based on europium(III) beta-diketonate complexes chemically bonded to functionalized polydimethylsiloxane. ChemistrySelect 2018;3:10491–501.

[15] Shakirova JR, Shevchenko NN, Baigildin VA, Chelushkin PS, Khlebnikov AF, Tomashenko OA, Solomatina AI, Starova GL, Tunik SP. Eu-based phosphorescence lifetime polymer nanothermometer: a nanoemulsion polymerization approach to eliminate quenching of Eu emission in aqueous media. ACS Appl Polym Mater 2020;2:537–47.

[16] Kitaura R, Onoyama G, Sakamoto H, Matsuda R, Noro S, Kitagawa S. Immobilization of a metallo Schiff base into a microporous coordination polymer. Angew Chem Int Ed 2004;43:2684–7.

[17] Routaray A, Nath N, Maharana T, Sahoo PK, Das JP, Sutar AK. Salicylaldimine copper(II) complex catalyst: pioneer for ring opening polymerization of lactide. J Chem Sci 2016;128:883–91.

[18] Nakamoto K, Wiley J, Sons. Infrared and Raman spectra of inorganic and coordination compounds. Part B; 1997.

[19] CCDC. CSD web interface. Cambridge, UK: Cambridge Crystallographic Data Centre, 12 Union Road; 2019.

[20] Hao L, Lu Y, He Z, Lau Q, Wang E. Synthesis, structure, and characterization of two 1-D homometallic coordination polymers based on carboxylate-functionlized salen ligands. J Coord Chem 2015;68:2682–90.

[21] Zhu C, Xuan W, Cui Y. Luminescent microporous metal–metallosalen frameworks with the primitive cubic net. Dalton Trans 2012;41:3928–32.

[22] Shintoyo S, Fujinami T, Matsumoto N, Tsuchimoto M, Wesalski M, Bienko A, Mrozinski J. Synthesis, crystal structure, luminescent and magnetic properties of europium(III) and terbium(III) complexes with a bidentate benzoateand a tripod N$_7$ligand containing three imidazole, [LnIII(H$_3$L)benzoate](ClO$_4$)·H$_2$O·2MeOH (LnIII=EuIII and TbIII). Polyhedron 2015;91:28–34.

[23] Sahoo J, Lakshmi DS, Subramanian PS, George TM, Reddy MLP. Synthesis, characterization and photo-physical properties of Eu(III) complexes and its luminescent thin films. Opt Mater 2017;70:83–91.

[24] Lapaev DV, Nikiforov VG, Lobkov VS, Knyazev AA, Galyametdinov YG. Reusable temperature-sensitive luminescent material based on vitrified film of europium(III) β-diketonate complex. Opt Mater 2018;75:787–95.

[25] Piccinelli F, De Rosa C, Melchior A, Faura G, Tolazzi M, Bettinelli M. Eu(iii) and Tb (iii) complexes of 6-fold coordinating ligands showing high affinity for the hydrogen carbonate ion: a spectroscopic and thermodynamic study. Dalton Trans 2019;48:1202–16.

[26] Sakai H, Kubota T, Yuasa J, Araki Y, Sakanoue T, Takenobu T, Wada T, Kawai T, Hasobe T. Protonation-induced red-coloured circularly polarized luminescence of [5]carbohelicene fused by benzimidazole. Org Biomol Chem 2016;14. 6738-674.

[27] Xu N, Wang RL, Li DP, Zhou ZY, Zhang T, Xie YZ, Su ZM. Continuous detection of HCl and NH$_3$ gases with a high-performance fluorescent polymer sensor. New J Chem 2018;42:13367–74.

[28] Jiménez R, Duarte F, Nuti S, Campo JA, Lodeiro C, Cano M, Cuerva C. Thermochromic and acidochromic properties of polymer films doped with pyridyl-β-diketonate boron(III) complexes. Dyes Pigments 2020;177:108272.